



P-350

## Enhancing gas field discovery by multicomponent imaging and joint inversion

*Xiao-gui Miao, Pu Wang and Yongxia Liu, CGGVeritas*

### Summary

The dramatically lateral lithological variations due to the complex fluvial sediments result to major challenges in the characterization of the highly permeable gas sandstones among the widely distributed less permeable sandstones in the Sulige gas field, located in the Erdos basin of China. Application of the multicomponent technology in the Sulige Basin aims at enhancing the possibility to discover high productive gas reservoirs. Directly extracting  $V_p/V_s$ , Poisson's ratio and other elastic parameters from multicomponent data provides a more accurate and straightforward way to delineate the characteristics of the sandstone gas reservoirs. However, the complicated near surface geological conditions including heterogeneity of the fluvial deposits associated with larger scale stratigraphic variability in the Sulige Basin impose serious challenges for multicomponent data processing and inversion. This paper shows a successful application of three-component seismic data in the Sulige gas field. Through the registration of the PP and PS equivalent reflection events and by building the initial velocity model, PP-PS joint inversion can provide inverted elastic parameters through both pre-stack angle gather and post-stack seismic data. It is concluded that the PP-PS joint inversion can reduce the drilling risks and effectively delineate the characteristics of the gas sand reservoir in the Sulige gas field.

### Introduction

Recently, multicomponent seismic exploration technology has been widely promoted in China. A successful application of the technology to distinguish true and false flat points through joint PP/PS inversion was reported in the Zunger Basin Northwest of China (Dang et al. 2009). It provided more information for reservoir characterization and fluid prediction. Since P and PS waves respond differently to gas reservoir, the first three-component 3D seismic survey in China was conducted in 2005 in the Sulige oil field of the Ordos Basin, with the objective to solve previously encountered technical difficulties and improve the forecast of highly productive gas reservoirs within less permeable sandstones. A previous study indicated a decreasing velocity ratio and lower Poisson ratios in the gas bearing sandstones in the area. The PP/PS joint inversion that makes use of the three component data is thus expected to provide more reliable and accurate information for gas reservoir characterization. A lot of effort was invested in processing the three-component data. Due to complicated near surface conditions, the quality of the previously processed PP and PS data did not meet the requirements for joint PP/PS inversion. The three-

component data have been re-processed and are now presented in this paper.

### Geology

The Sulige Gas field is located in a transition zone from deltaic to stream sedimentary systems. The gas reservoirs are composed of braided stream sandstone and shale sedimentary facies of the Shihezi Formation He8 section of the Lower Permian Group within the Upper Palaeozoic formation. The distribution and connectivity of the fluvial sandstones in a braided distributary channel system significantly impacts reservoir productivity. Well logs show that the thicknesses of sandstones with high porosity and permeability are usually less than 10 meters, even though the sandstones may be as thick as 20-30 meters.

### Data processing

The primary challenge in three-component data processing in the Sulige area arises from the complicated near surface geological condition. The Sulige area is well known to be full of sandy hillocks in the near surface, where there are deep valleys filled with quicksands lying in the terrain of



## Enhancing gas field discovery by multicomponent imaging and joint inversion



the large loess landforms, which cause huge variations in the thickness of the near surface low velocity zone and result in serious long and short wavelength statics problems in seismic profiles. Conventional refraction static methods cannot handle this problem. Near surface conditions also cause large lateral variations in seismic amplitude attenuation and low S/N ratio problems in the three component data. To overcome these problems, we have developed a strategy to process the P and PS wave data simultaneously from a slightly smoothed topographic surface. The processing flow includes turning wave tomography with well constraints for near surface velocity model and static corrections, P and PS wave double square root NMO corrections directly from the floating datum, surface consistent amplitude corrections with absorption compensation, noise and interbed multiple attenuation, surface consistent deconvolution, and prestack time migration.

**A) Process PP and PS data from topographic surface:** In order to account for elevation variations between the shot, receiver and common-midpoints (CMP) or common-conversion points (CCP), PP and PS data were processed (NMO corrected and migrated) from a floating datum, a slightly smoothed topographical surface. Due to the close proximity of the floating datum to the true elevation surface, differences between the traveltimes of the actual raypaths in the subsurface are decreased, thereby minimising travel time errors introduced by refraction statics. This is particularly helpful at the interpretation stage, as the PP and PS data were processed from the same floating datum, which also facilitated event correlation.

**B) Turning wave tomography and shear statics:** After carefully picking the first breaks and a near surface velocity model was estimated using ten iterations of tomographic inversion. A pseudo datum at a velocity equal to 2400m/s was used to calculate weathering statics for shots and receivers. Figure 1 shows the iso-velocity profile of the tomographic velocity model at velocity=2400m/s, the horizon depths are represented by colours, which vary in the range 0-400m. The velocity model clearly delineates near surface structural changes from the undulant hilly area in the east side of the survey to the ancient channel systems in the west side of the survey. It is used not only for statics calculation, but also for double square root NMO corrections from the smoothed topographic surface. Uphole information from 185 wells was employed to constrain the

tomo-statics solution as well. It is clear that layer-based refraction statics methods, such as GLI, certainly are not suitable for such large lateral structure changes.

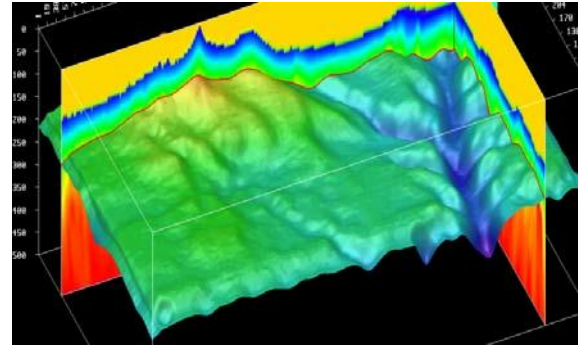
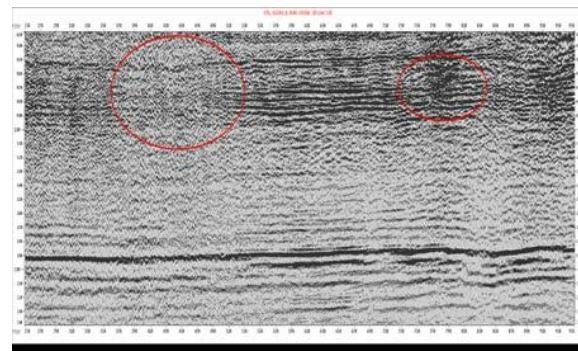


Figure 1. Shallow velocity model derived from turning wave tomography: The depth of an iso-velocity horizon (2400m/s), is shown using a color bar in 0-400m.

Figure 2 shows a comparison of statics applied by using a conventional GLI refraction statics method and the tomographic solution for P wave data. The turning wave tomo-statics certainly made significant improvements to the lateral continuity of reflection horizons. For the PS data, the shot-side P-wave statics were applied to the source-side first, and then receiver side shear statics were calculated by cross-correlation of a shallow horizon marker from the PP and PS receiver stacks and applied to the PS section. Figure 3 shows a PS wave stack comparison before and after shear wave statics application. Clearly, shear wave static values are quite large. Without shear-wave statics, the reflective horizons are not coherent. They are much improved after application of the shear wave statics.



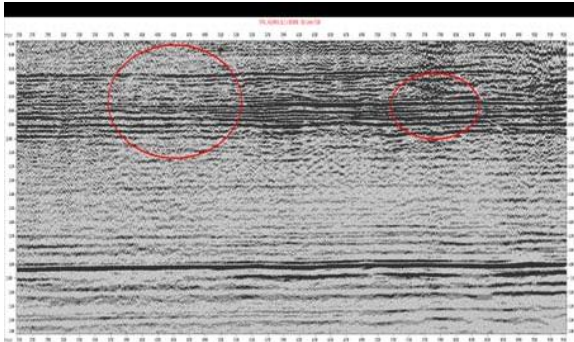


Figure 2. Comparison of P wave stack sections with statics calculated by the tomographic solution and the conventional GLI method: Top: with conventional GLI refraction statics; Bottom: with Tomo-statics.

**C) PS wave azimuthal anisotropic compensation:** There are evidences of shear-wave splitting on the horizontal components. After rotation to radial and transverse components, significant coherent signals are observed in the transverse component around 1.2s of PS time. The shear wave splitting analysis was carried out to derive the direction of anisotropic orientation axis and the delay times between fast and slow PS waves. The anisotropic correction based on the derived values has then been applied to the PS data. After anisotropic compensation, the signal on the transverse component is almost all rotated back to the updated radial component, and the energy splitting between the horizontal components due to shear wave birefringence has been compensated for.

**D) Amplitude compensation and noise attenuation:** As mentioned earlier, large lateral variations in the near surface also create uneven amplitude attenuation across the survey area. Q compensation and surface consistent amplitude corrections were performed to recover inconsistent amplitude decays and to remove footprint caused by the surface condition. Noise attenuation was also carried out, especially in the area of an ancient channel system which causes strong absorption and very low S/N ratio. Various types of noises, ground rolls, large abnormal spikes and air waves, heavily contaminate the data; these were attenuated using crossspread noise attenuation methods and adaptive ground roll modelling and subtraction (?). After tremendous efforts, high quality PP and PS data were obtained, with dominant frequencies around 45 Hz for the P wave prestack migrated data and 25 Hz for the PS prestack migrated data, respectively.

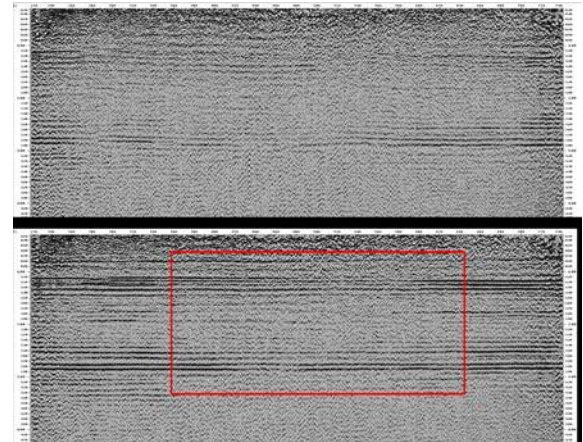


Figure 3. Comparison of receiver statics for PS wave stack section: Top: Radial component section before shear-wave statics application; Bottom: After shear-wave statics applied.

Figure 4 shows the final migrated PP and PS sections. The major reflection events match very well with each other. It is also possible to analyze the different reflection characteristics for the target zone on PP and PS data, respectively.

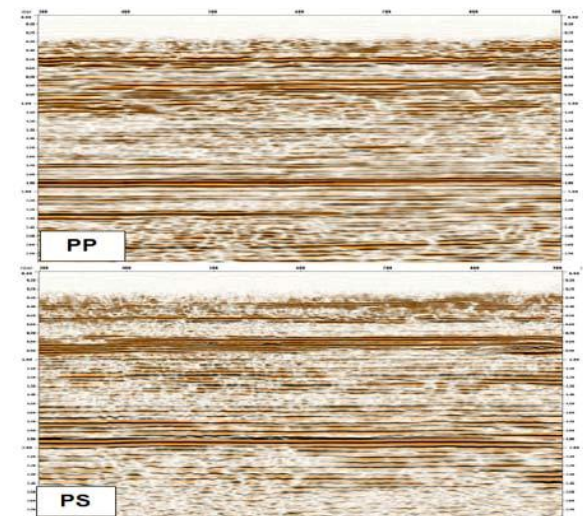


Figure 4. Prestack time migrations of PP and PS sections. The major reflection events between PP and PS sections match each other very well.

## PP/PS data event registration and joint inversion

The most critical step to ensure a successful joint PP/PS inversion is correct registration of P wave reflection events with their equivalent reflections on the PS data. Since the



two data have different frequency bands, we have applied a matching filter to the PP and PS data. Then the PP and PS event registration was carried out for the target zone. Three horizons were picked on both PP and PS sections in the target zone as shown in Figure 5.

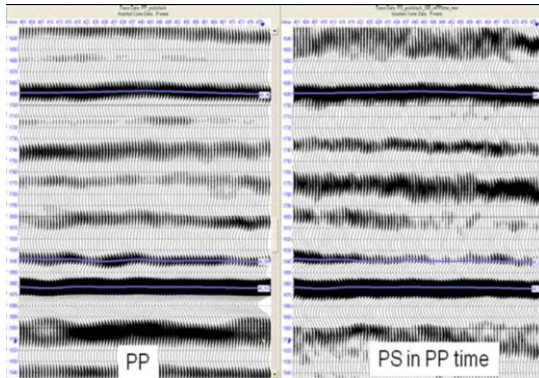


Figure 5. PP and PS reflection events registration: Three horizons were picked on both PP and PS data sections.

The joint PP and PS inversion scheme (Russell et al. 2005) is more accurate than one based on P wave data alone. However, in practice, the noise on both PP and PS prestack gathers also causes some difficulties in the inversion. The vertical  $V_p/V_s$  ratio from PP and PS travel time registration was used as an initial model and as a constrain in the joint PP and PS inversion. The details of the method are described in a separate paper (Zhao et al., 2011).

The PP/PS joint inversion derived elastic parameters from prestack angle gathers and poststack seismic data. Based on the inverted Poisson's ratio map within the target time window, we then calibrate the attributes with the existing drilling data. All the wells in Sulige gas field could be classified into three categories according to their production rates: Good (Class I, highly productive gas wells), Fair (Class II, productive gas wells) and Poor (Class III, less productive gas wells, or dry boreholes). Figure 6 marks all the available wells on the inverted Poisson's ratio map. It demonstrates that more than 81% of the wells are highly correlated with the inversion results.

### Conclusions

After comprehensive amplitude preserving PP and PS data processing through turning wave tomography, shear wave statics, Q compensation, noise and multiple attenuation, NMO correction and prestack migration from the floating datum, the effect of large lateral variations in near surface has been very well compensated for, which produced high quality PP and PS prestack migrated gathers and stacks and facilitated reliable registration of PP and PS reflection events. The Poisson's ratio from the PP/PS joint inversion correlates well with the drilling data, and proved to be useful in reducing drilling risks in the area and effectively delineate the characteristics of the gas sand reservoir in Sulige gas field.

### Acknowledgments

The authors would like to express special thanks to Sihai Zhang of Petroleum University of China and Linping Do, G. Kirtland Grech and Steve Roche of CGGVeritas for their help during the processing. They would like to thank the colleagues in CGGVeritas Technology Service (Beijing) Ltd. for their cooperation and support. In addition, the authors express special thanks to Brian Russell for his valuable comments and the management of both PetroChina and CGGVeritas for permission to publish this work.



## Enhancing gas field discovery by multicomponent imaging and joint inversion



"HYDERABAD 2012"

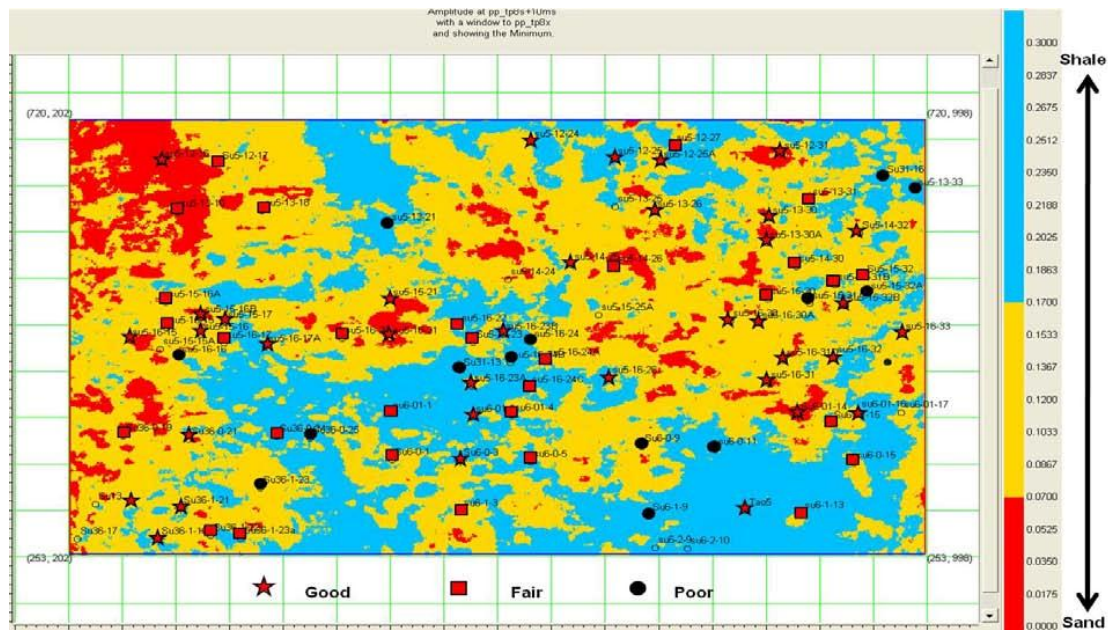


Figure 6. Poisson's ratio map for the whole survey. In total there are 80 wells (including the 4 wells involved in the inversion). Most of the drilling data is consistent with the derived Poisson's ratio map